Radar Backscatter Estimates From a Combined Ice Growth and Surface Scattering Model of First Year Sea Ice

R.H. Wade and W.F. Weeks

Geophysical Institute

P.O. Box 757320 – University of Alaska – Fairbanks, AK 99775-7320 – U.S.A.

R.H.W. (907)-474-6438 – fax (907)-474-5195 – rwade@iias.images.alaska.edu

W.F.W. (907)-474-7280 – fax (907)-474-7290 – willy@dino.gi.alaska.edu

ABSTRACT

A non-linear growth model which solves the surface energy balance and heat conduction equations was developed to estimate thermal and physical properties of sea ice. The model incorporates several mechanisms that effect the salinity profile including initial brine entrapment, brine expulsion and gravity drainage and is a non-linear extension of the model initially developed by Cox and Weeks (1988). The ice growth model was then coupled to a constant roughness surface backscattering model for radar. By calculating the average dielectric constant of the penetration depth and using this value in the backscattering model, a comparison of the predicted signature variations in first year sea ice was performed against observed backscattering values from ERS-1 SAR images of Dease Inlet. The agreement between calculated and observed backscatter was surprisingly good considering that other factors may also influence radar returns.

1. INTRODUCTION

Sea ice is a complex and dynamic substance which changes both in time and space. Its salinities alone range from as high as 20 ppt in newly-formed ice to near 0 ppt in the upper portion of old multiyear floes. The exact values are effected by a variety of processes including the amount of salt initially entrapped, brine expulsion, gravity drainage, brine pocket migration, and if the ice survives a melt season, by flushing (Weeks and Ackley, 1986). An accurate radar backscattering model for sea ice would require a detailed description of the physical properties and their response to the atmospheric and oceanic forcing which they encounter. The characterization would include changes in brine volume, salinity and temperature of the layers influenced by the radar radiation and is only practical with the use of a comprehensive sea ice model.

2. ICE GROWTH MODEL

The ice growth and properties model utilized is an extension and combination of several different earlier models. The surface energy balance routine is based on work of Untersteiner and Maykut (1971) and Maykut (1978). The ice property routines, such as brine volume, brine salinity, bulk salinity, brine expulsion, gravity drainage and ice densities are based on work by Cox and Weeks (1975; 1988). The non-linear temperature profile and the position of the freezing interface is determined by the finite-difference model that was developed for geothermal problems by Goodrich (1974). The initialization of the growth rate for the first layer utilizes the empirical ice growth relations of Bilello (1961), while the thermal properties such as latent heat, thermal conductivity and thermal capacitance are based on work by Schwerdtfeger (1963), Ono (1975) and Yen (1981).

The ice growth program has five major parts: 1) an initialization of the first layer, 2) a calculation of the surface energy balance, 3) a determination of the properties of the ice at different levels in the ice sheet, 4) a treatment of the different aspects of the desalination process, and 5) a finite-difference routine to estimate the changes in the temperature profile and growth rate.

Initialization

The user specifies the number of days of ice growth, the starting day relative to September 1. The program then reads the meteorological conditions (air temperature, wind speed and snow fall) for the site under study and determines the air temperature for the first freezing day. It then estimates the growth rate for the initial layer of ice by determining the freezing degree-day equivalent of one time step (1/2 hr) for the first freezing day (relative to -1.8°C) and estimates, the amount of ice that will grow in that time, thereby establishing an initial estimated growth rate. From this growth rate, the initial salinity may be determined and the surface energy balance calculated. The surface energy balance determines the surface temperature of the ice allowing the program to calculate the brine volume, the thermal conductivity, the latent heat and the heat capacitance for that layer (Yen 1981). After the initialization of the first layer has been completed, the program continues on through the normal program loop with the exception of the desalination process which only occurs if there are at least two layers (2 cm) of ice present.

Surface Energy Balance

The ice surface temperature is determined by the surface energy balance equation via the use of an iterative procedure. The air temperature, wind speed and snow thickness are input from a file. The incoming shortwave radiation, the incoming longwave radiation and the relative humidity, for each day, are estimated from a smoothed data set. Variations in the albedo as a function of ice thickness are estimated from the field measurements of Weller (1972). The latent heat flux is then related to the surface temperature through the specific humidity (Maykut 1978). The emitted longwave radiation, the latent heat flux, the sensible heat flux and the conducted heat flux, are then iterated as a function of the ice surface temperature until the surface energy equation is balanced.

Ice Properties

The ice properties routine first determines the snow cover and then calls the surface energy balance routine to determine the ice surface temperature. The program calculates the growth velocity from the ice thickness and the amount of time it took to grow the new layer. It then determines the initial salt entrapment and calculates the average temperature of the new layer. Using the average temperature and the initial salt entrapped, the brine salinity and the brine volume are determined and the latent heat and the heat capacity of the new layer are calculated.

Desalinization

If the program has grown more than two layers of ice, desalination of the layers above the new layer is initiated. For each layer above the new layer, the desalination process determines the average temperature of that layer. It also recalls the average temperature of that layer the last time desalination was called. It then uses this temperature change to determine the brine salinity and brine volume change, and calculates the salinity change due to brine expulsion. The salinity of the layer is then adjusted with the expulsed brine going to the layer, either above or below, containing the higher brine volume.

The temperature gradient between the layers, the brine volume and the time since last desalination are used to calculate the salinity change due to gravity drainage. When the gravity drainage from the layer above is larger than the gravity drainage of the current layer, the difference is added to the current layer. After the thermal properties of all the layers are updated, the program enters the finite-difference routine and continues to grow ice until the number of target days has been reached.

3. FINITE-DIFFERENCE PROCEDURE

The normal program loop calls a finite-difference routine that solves the Stefan Problem of heat conduction involving a phase change. This is accomplished by substituting the moving boundary condition of the phase change interface with an apparent latent heat source term added to the heat conduction equation. The program then uses a forward looking and a backward looking Gaussian elimination process to localize the phase change interface between two nodes. For the element containing the ice-seawater interface, the routine uses a technique that follows the position of the moving interface and maintains the nonlinearity of the problem (Goodrich 1978).

The finite-difference model is initialized with the first layer of ice having the thermal properties calculated during the initialization procedure. The remaining layers are assumed to have the thermal properties of a mixture of ice and sea water in a ratio of 1:3 at a temperature of -1.8°C. The program steps through each time step of 1/2 hour, locating the freezing interface and establishing the temperatures at each node. After each time step, the ice thickness is checked and the program calculates the snow thickness, determines the ice surface temperature for the next iteration and updates the ice properties for all layers.

4. GROWTH MODEL RESULTS

In the following section, the growth model will be used to examine some of the complex inter-relations between the meteorological conditions, the amount of ice grown, and the resulting sea ice properties. Although the large scale feedbacks on a regional to global scale between sea ice and climate parameters have recently received considerable attention in the literature, it is well to note that the "simple" problem of sea ice growth also contains complex feedbacks, although on a local scale. The following figures (Figures 1 and 2) show the predicted temperature, salinity and brine volume profiles for first year sea ice "grown" via the growth model using the meteorological inputs for Point Barrow, Alaska as representative of the nearby Dease Inlet as discussed above.

In Figure 1 the ice was allowed to grow for 200 days beginning on 10 October 1991 (day 40) and ending on 8 May 1992 (day 240). As this was approximately the maximum length of time sea ice could have grown during this year, the resulting ice thickness of 176 cm can be taken as representing a maximum first year ice profile for this region. Note the non-linear temperature profile with a warming temperature wave propagating downward. This figure will be referred to again in the section on the radar backscatter of sea ice.

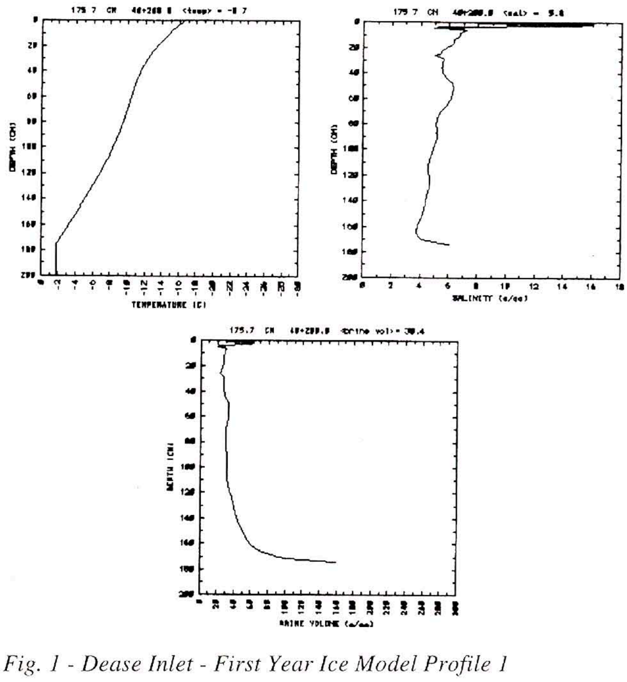

Fig. 1 - Dease Inlet - First Year Ice Model Profile 1

The next figure (Figure 2) shows the temperature, salinity and brine volume profiles for the same date (8 May 1992) for ice that began growing 39 days later on 18 November 1991 (day 78). When comparing these plots, the most marked difference is observed in the salinity profile. The more rapid growth rate of the ice that initially formed in November, as a result of the lower temperatures in November (-30°C) than in October (-14°C), caused an increase in the initial salt entrapment in the ice resulting in high salinity and brine volumes in the upper layers of the November ice sheet. This decreased the thermal conductivity of these layers and ultimately slowed the growth of this particular ice sheet.

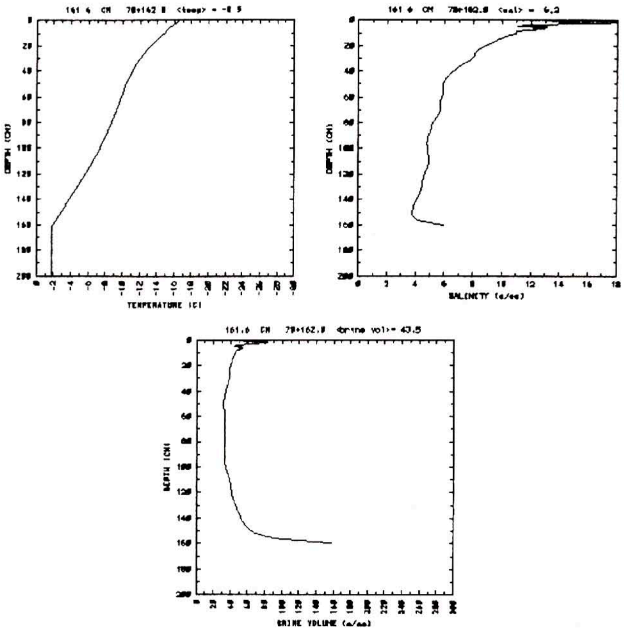

Fig. 2 - Dease Inlet - First Year Ice Model Profile 2

5. RADAR BACKSCATTERING MODEL

The C-band SAR on the ERS-1 satellite is a active microwave radar operating at a wavelength (SYMBOL 108 \f "Symbol") of 5.6 cm with vertical transmit and receive polarization (VV). The microwave signature is the result of the two basic scattering mechanisms, surface and volume scattering. For surface scattering: a) the scattering strength is proportional to the relative complex dielectric constant of the surface and b) its angular scattering pattern is governed by the surface roughness. For volume scattering: a) the scattering strength is proportional to the dielectric discontinuities and the density of these inhomogeneities within the medium and b) its angular scattering pattern is determined by the roughness of the boundary surface, the average dielectric constant of the medium and the geometric size of the inhomogeneities relative to the incoming wavelength.

Penetration Depth

One method to determine the relative contribution of surface scattering and volume scattering is to calculate the depth of penetration of the radar pulse. The depth of penetration is a measure of the "active layer" of the medium which is sea ice in our case and is the depth to which the radiation may penetrate and still give a signal return that is discernible. The depth of penetration ($\delta = 1/2\ \alpha$) is defined as the depth at which the power falls to 1/e of the power at the surface of the medium. The field attenuation coefficient α is generally defined as

$$\alpha = \frac{2\pi}{\lambda_0}[\mathrm{Im}(\sqrt{\varepsilon})]$$

where $\varepsilon = \varepsilon_1 - i\varepsilon_2$ is the relative dielectric constant and $\lambda = 5.6$ cm is the radar wavelength of the ERS-1 SAR. The imaginary part of the square root of the complex dielectric constant ($\sqrt{\varepsilon}$) is equal to

$$\mathrm{Im}(\sqrt{\varepsilon}) = (\varepsilon_1^2 + \varepsilon_2^2)^{\frac{1}{4}} \times \left\{ \sin\left[\frac{\tan^{-1}\left(\frac{\varepsilon_2}{\varepsilon_1}\right)}{2}\right]\right\}$$

The primary parameter for influencing the dielectric constant in sea ice is the brine volume (Vant et al. 1978). An expression for the relative dielectric constant (for the 5.3 Ghz C-Band radar) as a function of brine volume (V_b) may be calculated utilizing the equations by Kim (1984) and Vant (1978)

$$\varepsilon_1 = [0.995 - 0.00154 \times (5.3)]\varepsilon_1'$$
$$\varepsilon_2 = [0.914 - 0.00546 \times (5.3)]\varepsilon_2'$$

where the brine volume dependence of the coefficients is

$$\varepsilon_1' = 3.05 + 7.20 \times V_b$$
$$\varepsilon_2' = 0.024 + 3.29 \times V_b$$

Sea Ice Backscattering Model

Neglecting any surface and volume interactions, the bistatic scattering coefficient may be broken down into its surface scattering and volume scattering components and treated as a combination of these two effects. For sea ice, the total radar backscattering coefficient may be represented by the following equation

$$\sigma^0 = \sigma_s^0 + Y^2(\theta)\left[\sigma_v^0 + \frac{\sigma_i^0(\theta')}{L^2(\theta')}\right] \qquad (1)$$

where σ_s^0 is the backscattering coefficient due to the surface scattering, Y (θ) is the one way power transmissivity, σ_v^0 is the volume scattering,$\sigma_i^0$is the backscatter from the ice-water interface, and L (θ') is the one way loss factor and is equal to

$$L(\theta') = \exp\left(\kappa_e d \frac{1}{\cos\theta}\right)$$

where d is the layer thickness, θ is the incidence angle and κe is the extinction coefficient.

As the freezing interface of sea ice is dendritic structure with a negligible scattering coefficient, the interface scattering term of the backscattering coefficient for sea ice may be neglected and equation (1) may be written as

$$\sigma^0 = \sigma_s^0 + Y^2(\theta)\sigma_v^0$$

Here the one way power transmissivity ($Y(\theta)$) is equal to

$$Y(\theta) = 1 - |R(\theta)|^2$$

The backscattering coefficient for a "slightly rough" (Ulaby et al. 1986) surface may be represented by the equation

$$\sigma_s^0 = 8\, k^4 \sigma^2 \cos^4\theta \times |R(\theta)|^2 \times W(2k \sin\theta, 0)$$

where σ is the standard deviation of the surface roughness, W(2ksinθ, 0) is the Fourier transform of the surface correlation coefficient or the normalized roughness spectrum, and $|R(\theta)|^2$ is the complex Fresnel reflection coefficient. This corresponds to a surface with the standard deviation divided by the correlation length being less than 0.2 and a surface standard deviation less than 5% of the radar wavelength or for C-band radar $\sigma < 0.3$ cm and $\ell > 1.5$cm.

For a surface with an isotropic roughness spectrum or Gaussian correlation coefficient with correlation length l and wave number $k = \frac{2\pi}{\lambda}$ this equation may be rewritten as

$$W(2\,k \sin\theta, 0) = \frac{\ell^2}{2}\exp\left[-(k\,\ell \sin\theta)^2\right]$$

The Fresnel reflection coefficient is given by

$$|R(\theta_r)|^2 = \frac{\left[\cos\theta_r - \sqrt{r}\cos\left(\frac{\theta}{2}\right)\right]^2 + r\sin^2\left(\frac{\theta}{2}\right)}{\left[\cos\theta_r - \sqrt{r}\cos\left(\frac{\theta}{2}\right)\right]^2 + r\sin^2\left(\frac{\theta}{2}\right)}$$

where

$$\theta = \tan^{-1}\left[\frac{\varepsilon_2}{\varepsilon_1 - \sin^2\theta_r}\right]$$

$$r = \left\{\left[\varepsilon_1 - \sin^2\theta_r\right]^2 + \varepsilon_2\right\}^{\frac{1}{2}}$$

and θ_r is the angle of incidence and ε_1 and ε_2 are the real and imaginary part of the complex dielectric constant.

Inserting these expressions into the equation for the surface backscattering coefficient leads to

$$\sigma_s^0 = 8\,k^4\,\sigma^2\cos^4\theta \times |R(\theta)|^2 \times \frac{\ell^2}{2}\exp\,[k\,l\sin\theta)^2]$$

For a given surface with standard deviation σ and correlation length ℓ, the only parameter in this equation that is independent of the surface geometry is the complex Fresnel reflection coefficient. Therefore for a given surface, this equation may be rewritten as

$$\sigma_s^0 = A \times |R(\theta)|^2$$

where θ is the incidence angle and A is a constant whose value depends upon the surface geometry and the incidence angle and may be determined for each radar image.

The second term in the radar return is the volume backscattering coefficient which may be represented by the following equation

$$\sigma_v^0(\theta') = \frac{N\,\sigma_b\cos(\theta')}{2\,\kappa_e}\left[1 - \frac{1}{L^2(\theta')}\right]$$

In this expression N is the number of scatterers per unit volume (all assumed to be identical), σ_b is the backscattering cross-section of one scatterer, κ_e is the extinction coefficient of the scattering layer, and $L^2(\theta')$ is the two way loss factor indicative of the medium. The loss factor may be represented by

$$L^2(\theta') = [\exp\,(\kappa_e\,d\sec\theta)]^2$$

where d is the layer thickness, κ_e is the extinction coefficient and θ is the incidence angle.

In general, the volume scattering term for first year sea ice is relatively small due to the small penetration depths when compared to the surface scattering term. This is not the case for multiyear ice where the volume term actually dominates the radar return and this model fails. However, for first year sea ice the volume scattering term may be replaced by a constant and the equation for the volume backscattering coefficient becomes

$$\sigma_s^0(\theta) = B$$

where B is the constant term.

Substituting the expressions for the surface scattering term and the volume scattering term into the total radar backscattering equation for sea ice above, leads to the equation

$$(\theta) = 8k^4\sigma^2\cos^4\theta \times |R(\theta)|^2 \times \frac{\ell^2}{2}\exp[-(k\ell\sin\theta)^2] + Y^2(\theta) \times \frac{N\sigma_b\cos(\theta')}{2\kappa_e} \times \left\{1 - \frac{1}{\left[\exp\left(\frac{\kappa_e d}{\cos\theta}\right)\right]^2}\right\} \tag{2}$$

where the first term is the surface scattering contribution and the second is that due to volume scattering. Making the assumptions about each term as in the previous sections the equation becomes

$$\sigma^0 = A \times |R(\theta)|^2 + B \times [1 - |R(\theta)|^2]^2$$

or

$$\sigma^0 = B \times |R(\theta)|^4 + (A - 2B) \times |R(\theta)|^2 + B$$

For values of $R(\theta) < 1$ this equation may be represented by

$$\sigma^0 \approx C \times |R(\theta)|^2 + D$$

This form of equation 2 using assumptions based on work by Kim, et al. (1985) was first formulated by Soulis et al. (1989).

The theoretical sea ice backscattering model uses the output of the ice physical properties from the ice growth model to determine the penetration depth as outlined in the introduction section. It then determines the average ice properties for a layer whose thickness is equal to the penetration depth and uses these characteristics to calculate the predicted backscattering coefficient.

The values for C and D were established from ERS-1 SAR measurements of first year ice in the Dease Inlet area near Point Barrow, Alaska. First, images from 4 September 1991 to 7 June 1992 were radiometrically corrected and backscattering values were noted from a representative area of first year ice. Next, the mean and variance of these measurements were calculated and compared to the mean and variance of the predicted Fresnel coefficients. Then, the values for the constants C and D were adjusted to scale and translate the predicted values to match the range and mean of the measured values. The resulting values were C = 188.9 dB and D = -35.0 dB

6. SAR MODEL RESULTS

To determine the usefulness of this technique, it was important to obtain, over a nearly complete ice growth season, SAR images of sea ice whose thicknesses were fairly well known, and where meteorological conditions were measured during the greater portion of the ice growth season. The Dease Inlet area east of Point Barrow Alaska seemed like a reasonable candidate in that the barrier islands just north of the inlet trapped the ice, allowing the thermal history to be documented while the meteorological station at Barrow (approximately 50 km to the west) collected the required meteorological data. While the exact thickness of the ice growing in the Dease Inlet was not known, a reasonable estimate can be obtained from the ice growth model and from past field experience in this region.

Figure 3 shows the relevant radar characteristics of the growing sea ice at Dease Inlet from 10 October 1991 to 28 April 1992. The physical properties of this ice sheet on 8 May 1992 may be seen in figure 2. The values of the penetration depth, brine volume and temperature are those of the "active layer" as described earlier and represent the value for any given day. It should be noted that the backscatter values (σ^0) are plotted against theoretical thickness rather than days of growth. Because there was no melting, each day has associated with it a unique theoretical thickness associated with it.

ERS-1 SAR images were obtained for the Dease Inlet/Point Barrow area covering the time period mentioned above, except for a period during December 1991 when the satellite orbit was altered. These images were corrected radiometrically to eliminate differences in processor gain, system noise and variations in antenna pattern. A comparison with the measured values from this area with the predicted values generated by the model is shown in figure 4.

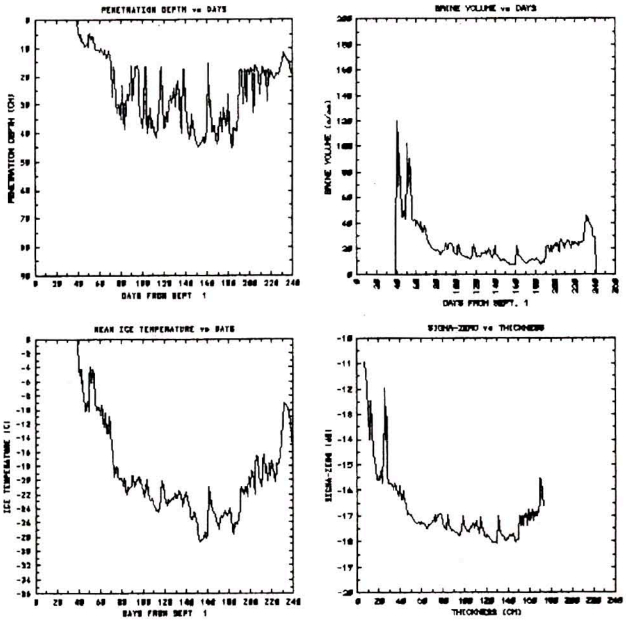

Fig. 3 - Dease Inlet - Backscattering Profile

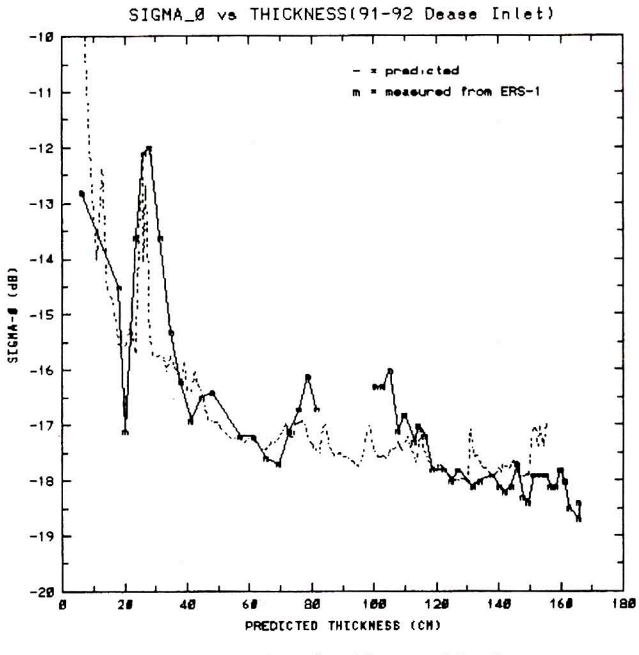

Fig. 4 - Dease Inlet - Predicted vs Measured Backscatter

7. CONCLUSIONS

The radar backscattering model for first year sea ice that was developed in this article was based on the assumptions of a constant roughness surface and a strong dielectric dependence on brine volume. Using the calculated physical properties of the ice growth model, the penetration depth for C-band radar was determined and the active layer dielectric constant was input to the surface scattering model to produce predicted σ^0 values for first year sea ice. The comparison of the predicted first year ice σ^0 values to those obtained from ERS-1 SAR images of landfast ice at Dease Inlet proved to be surprisingly good considering the assumptions of the model. The large variations in the backscatter were strongly correlated to changes in the dielectric constant caused by the high sensitivity of the brine volume to temperature and desalinization. Thus, SAR imagery indirectly senses the thermal state of first year sea ice and the possibility of detecting an ice thickness signal through the brine volume sensitivity becomes real. However, while the high sensitivity to temperature opens the possibility of a thickness signal, the large variations in thermal forcing as a result of changing meteorological conditions tend to mask the signal behind a noisy background making retreival difficult.

The agreement between the predicted σ^0 values and the observed values, although generally satisfactory, showed marked differences in areas where the model clearly failed. A clear example of this may be seen late in the season when the ice temperature begins to rise. The discrepancy in signals during this general warming may be due to the presence of liquid water in the snow layer which has the effect of dramatically decreasing radar backscatter. The use of a more sophisticated backscattering model which incorporates the effects of liquid water in the snow layer as well as a more extensive treatment of volume scattering would undoubtedly increase the applicability and hopefully increase the effectiveness of the current model.

REFERENCES

Bilello M.A., 1961, Formation, growth and decay of sea-ice in the Canadian Arctic Archipelago. Arctic, 14(1): pp. 2-24.

Cox G.F.N. & Weeks W.F., 1975, Brine drainage and initial salt entrapment in sodium chloride ice. CRREL Research Report 345, Cold Regions Research and Engineering Laboratory, Hanover, New Hampshire. 85 pp.

Cox G.F.N. & Weeks, W.F., 1988, Numerical simulations of the profile properties of undeformed first-year sea ice during the growth season. Journal of Geophysical Research, 93(C10): pp. 12449-12460.

Goodrich L.E., 1974, A one-dimensional numerical model for geothermal problems. Technical Paper No. 421, National Research Council of Canada, Division of Building Research, Ottawa.

Kim Y.S., Moore, R.K. Onstott R.G. & Gogineni S., 1985, Towards identification of optimum radar parameters for sea ice monitoring. Journal of Glaciology, 31(109): pp. 214-219.

Maykut G.A., 1978, Energy exchange over young sea ice in the Central Arctic. Journal of Geophysical Research, 83(C7): pp. 3646-3658.

Maykut G.A. & Untersteiner N., 1971, Some results from a time-dependent thermodynamic model of sea ice. Journal of Geophysical Research, 76(6): pp.1550-1575.

Ono N., 1975, Thermal properties of sea ice IV. Thermal constants of sea ice. Low Temperature Science, Ser. A(26): pp. 329-349.

Schwerdtfeger P., 1963, The thermal properties of sea ice. Journal of Glaciology, 4(36): pp. 789-807.

Soulis E.D., Lennox W.C. & Sykes J.F., 1989, Estimates of the thickness of undeformed first year ice using radar backscatter. International Geosciences and Remote Sensing Symposium (IGARSS'89), 4: pp.2366-2369.

Ulaby F.T., Moore R.K. & Fung, A.K., 1986, Microwave Remote Sensing: Active and Passive, Volume III. Artech House, Norwood, Mass. 2162 pp.

Vant M.R., Ramseir R. O. & Makios V., 1978, The complex dielectric constant of sea ice at frequencies in the range 0.1-40 Ghz. Journal of Applied Physics, 43(3, part 1): pp. 1264-1280.

Weeks W.F. & Ackley, S.F., 1986, The growth, structure and properties of sea ice. In "The Geophysics of Sea Ice" (N. Untersteiner, ed.) NATO Advanced Study Institutes, Series B: Physics 146, Plenum Press, New York, pp. 9-164.

Weller G., 1972, Radiation flux investigation. The AIDJEX Bulletin, 14: pp. 28-30.

Yen Y.-C., 1981, Review of the thermal properties of snow, ice and sea ice. CRREL Report 81-10, Cold Regions Research and Engineering Laboratory, Hanover, New Hampshire. 27 pp.